NeuroImage 299 (2024) 120838

Contents lists available at ScienceDirect

NeuroImage

journal homepage: www.elsevier.com/locate/ynimg

Pre-supplementary motor area strengthens reward sensitivity in intertemporal choice

Gizem Vural, Natasha Katruss, Alexander Soutschek *

Department for Psychology, Ludwig-Maximilians-Universität Munich, Munich, Germany

ARTICLE INFO

Keywords:
Transcranial magnetic stimulation
Impulsiveness
Drift diffusion model
Computational modelling
Decision making

ABSTRACT

Previous investigations on the causal neural mechanisms underlying intertemporal decision making focused on the dorsolateral prefrontal cortex as neural substrate of cognitive control. However, little is known, about the causal contributions of further parts of the frontoparietal control network to delaying gratification, including the pre-supplementary motor area (pre-SMA) and posterior parietal cortex (PPC). Conflicting previous evidence related pre-SMA and PPC either to evidence accumulation processes, choice biases, or response caution. To disentangle between these alternatives, we combined drift diffusion models of decision making with online transcranial magnetic stimulation (TMS) over pre-SMA and PPC during an intertemporal decision task. While we observed no robust effects of PPC TMS, perturbation of pre-SMA activity reduced preferences for larger over smaller rewards. A drift diffusion model of decision making suggests that pre-SMA increases the weight assigned to reward magnitudes during the evidence accumulation process without affecting choice biases or response caution. Taken together, the current findings reveal the computational role of the pre-SMA in value-based decision making, showing that pre-SMA promotes choices of larger, costly rewards by strengthening the sensitivity to reward magnitudes.

1. Introduction

Decisions entailing trade-offs between rewards and their associated costs (e.g., trade-offs between reward magnitudes and the time until reward delivery in intertemporal choice) are thought to rely on interactions between a frontoparietal control network and the dopaminergic reward system (Frost and McNaughton, 2017; McClure et al., 2004; van den Bos et al., 2014). Neuroscientific research on the contribution to the frontoparietal control network to intertemporal choice has mainly focused on the dorsolateral prefrontal cortex (DLPFC), which was linked to a larger tolerance for waiting costs (Smith et al., 2018; Wesley and Bickel, 2014; Yang et al., 2018). Little is known, however, about the contributions of further parts of the frontoparietal control network to cost-benefit decisions. Both the pre-supplementary motor area (pre-SMA) and the posterior parietal cortex (PPC) show enhanced activation during intertemporal decisions (Rodriguez et al., 2014; van den Bos et al., 2014; Wesley and Bickel, 2014), but it remains unknown as to whether – and if so, how – these regions causally influence intertemporal decisions. The main goal of the current study therefore was to determine the causal roles of pre-SMA and PPC for cost-benefit decision making in intertemporal choice.

For a better understanding of these regions' contributions to decision making, we employed drift diffusion models (DDMs) of intertemporal choice. While most neuroscientific research on intertemporal choice focused on preferences for delayed versus immediate rewards deferred from binary choices, DDMs posit that intertemporal choices emerge from a decision process that can be divided into several subcomponents (Ratcliff et al., 2016). In particular, decision makers accumulate evidence for the choice options by integrating the weighted benefits and costs (drift rate) until the evidence for one option over the other reaches a threshold (decision boundary) (Soutschek and Tobler, 2023; Wagner et al., 2020). The starting point of the evidence accumulation process can be shifted towards one of the decision boundaries depending on a decision maker's bias towards larger-later (LL) or smaller-sooner (SS) rewards (starting bias). Such DDMs enable deeper insights into the computational roles of brain regions than the analysis of binary choice data, as they provide insights into the subcomponent of the decision process that is implemented by a brain region (Soutschek et al., 2023). Crucially, it is still controversially debated how pre-SMA and PPC influence the decision process. Previous studies suggest the pre-SMA to

* Corresponding author at: Department for Psychology, Ludwig-Maximilians-Universität Munich, Leopoldstr. 13, 80802 Munich, Germany.
E-mail address: alexander.soutschek@psy.lmu.de (A. Soutschek).

https://doi.org/10.1016/j.neuroimage.2024.120838
Received 27 May 2024; Received in revised form 3 September 2024; Accepted 4 September 2024
Available online 5 September 2024

modulate decision boundaries (i.e., the amount of evidence that is accumulated before a choice is made) in perceptual decision making (Berkay et al., 2018), but the pre-SMA was also linked to shifts in the starting bias (McIntosh and Sajda, 2020). In the domain of value-based choice, the pre-SMA was reported to encode the accumulated evidence for the choice options (Arabadzhiyska et al., 2022; Pisauro et al., 2017; Rodriguez et al., 2014). Likewise, also the lateral PPC was linked to evidence accumulation (Yu et al., 2020; Zhang et al., 2022), whereas other studies questioned such a role (Erlich et al., 2015; Krueger et al., 2017). Taken together, it remains unclear how PPC and pre-SMA causally influence the decision process underlying value-based choice.

Here, we aimed at elucidating the causal contributions of pre-SMA and PPC to value-based decision making by combining a DDM of intertemporal choice with timing-specific online transcranial magnetic stimulation (TMS). Healthy young participants made choices between smaller-sooner (SS; e.g., 4 euro today) and larger-later (LL; e.g., 5 euro in 90 days) monetary rewards while receiving TMS over pre-SMA or PPC either at an earlier (shortly after option presentation and thus during the non-decision time) or a later stage (during evidence accumulation and time-locked to individual decision times) of the decision process. This timing enabled us to investigate TMS effects on different stages of the choice process: The starting bias towards SS or LL options should be affected by early, but not late, TMS, whereas only late TMS pulses should modulate decision boundaries (amount of evidence required for making a choice). Drift rates during evidence accumulation, in contrast, should be susceptible to both early and late TMS effects due to the after-effects of early TMS pulses during the non-decision time (Taylor et al., 2011; Taylor et al., 2007; Thut et al., 2011). We hypothesized disruption of both pre-SMA and PPC activation – as belonging to the frontoparietal control network – to lead to more impulsive decisions. We then used hierarchical Bayesian drift diffusion modelling to determine the subcomponents of the decision process underlying the hypothesized roles of pre-SMA and PPC for intertemporal choices. While our findings provide no evidence for a causal contribution of the PPC to intertemporal decision making, they suggest the pre-SMA to moderate the influence of reward magnitudes on the evidence accumulation process, clarifying the computational role of the pre-SMA for cost-benefit decision making.

2. Materials and methods

2.1. Participants

A total of 32 volunteers (mean age: 26 years, range 20–36 years, 16 females) were recruited via internal participant pools. A power analysis based on the effect size of Cohen's d = 0.71 reported by a meta-analysis of TMS effects on intertemporal choice (Yang et al., 2018) suggests that 28 participants are sufficient to detect a significant effect (alpha = 5%) with a power of 95%. Participants were excluded from the study if they met any of the following criteria: a history of psychological or neurological disorders (including familial predisposition to epilepsy), increased intracranial pressure, history of craniocerebral trauma, infarctions, or neurosurgical interventions. Participants were ineligible if they were on any psychoactive medication, pregnant, had metal objects in the head area (with the exception of dentures or permanent retainers), implanted pump systems, neurostimulators, or cardiac pacemakers.

2.2. Ethics statement

The study was appoved by the ethics committee of the psychology department at the Ludwig-Maximilians-University Munich. Participants gave voluntary informed consent prior to participation and were compensated with 15 euro/hour plus a choice-dependent bonus.

2.3. Stimuli and task design

Participants performed an intertemporal decision task where they had to choose between smaller-sooner (SS; e.g., €3 today) and larger-later (LL; e.g., €5 in 90 days) monetary rewards (Fig. 1A). We used six levels for the reward magnitudes of the SS option (€1, €2, €3, €3.5, €4, and €4.5), while the amount of the LL option was fixed to €5 (Kapetaniou et al., 2021). The delays for the SS option varied from 0–40 days and from 10–180 days for the LL option, resulting in 10 different delay combinations (0 vs. 10 days, 0 vs. 20 days, 0 vs. 40 days, 0 vs. 90 days, 0 vs. 180 days, 10 vs. 40 days, 10 vs. 90 days, 10 vs. 180 days, 40 vs. 90 days, and 40 vs. 180 days). On each trial, participants were presented with pairs of monetary rewards on the left and right screen side for 3 seconds and asked to choose the option they preferred by pressing the left and right arrow keys (for the left and right choice option, respectively) on a standard keyboard. Trials were separated by an inter-trial interval of 2 seconds. To increase task engagement, we informed participants that at the end of the experiment we would randomly select one of their choices and pay them the chosen amount after the given delay via mail if a LL reward was chosen (SS rewards were paid out together with the participant fee directly after the experiment). While we timed the delivery of the bonus such that participants should receive it after the correct delay, we note that we cannot exclude some minor variation in the exact delivery date and potential influences of this procedure on participants' choices.

2.4. TMS protocol

TMS was administered using a MAG & More PowerMAG ppTMS stimulator equipped with a flat, Fig.-of-eight PowerMAG double coil PMD70 (2 × 70mm diameter). For accurate delivery of TMS pulses to the targeted brain regions, we employed neuronavigation using Brainsight software (v2.4.9; Rogue Research Inc). For this purpose, we collected T1-weighted structural MRI scans for each participant before the main experimental session (unless volunteers already possessed a structural scan from a prior MRI experiment). Anatomical brain images were obtained using a 64-channel head coil with the magnetisation-prepared rapid gradient-echo (MPRAGE) sequence, using the following parameters: 176 sagittal slices with a slice thickness of 0.8 mm, a repetition time (TR) of 1900 ms, an echo time (TE) of 2.2 ms, a flip angle of 9°, and a field of view (FOV) of 200 × 200 mm. We used these structural images to individually determine the pre-SMA (x = 6, y = 15, z = 58 (Rochas et al., 2013)) and PPC (x = 48, y = -52, z = 52 (Rodriguez et al., 2014)) TMS sites by warping the MNI coordinates for the pre-SMA and the PPC into the individual image space with the normalization routines implemented in SPM12. After the experiment, we asked participants verbally whether they perceived pre-SMA or PPC TMS as more aversive, and they reported no systematic differences.

During performance of the intertemporal decision task, we used Brainsight neuronavigation sofware to place and hold the TMS coil accurately over the pre-SMA and PPC target sites. We held the coil stable over the target site during all trials of a block, including no TMS trials. In an online TMS design, 10 Hz trains of four pulses were delivered with an intensity of 110% of the resting motor threshold (the last pulse was thus delivered 300 ms after the first pulse). The resting motor threshold was defined as the lowest intensity where single TMS pulses delivered to the left primary motor cortex led to observable twitches of the contralateral hand in 5 out of 10 trials. TMS trains were delivered at three different timings: no TMS, early TMS, and late TMS. Early TMS pulses were administered 100, 200, 300, and 400 milliseconds after onset of the decision screen. Timing of late TMS pulses was calibrated to individual decision times such that the final pulse coincided with an individual's median decision time. The rationale for administering TMS during early versus late periods of the decision process was that only early TMS pulses should affect the general bias for LL or SS rewards (starting bias parameter in the framework of DDMs; see below), whereas late TMS might show stronger effects on decision boundaries (amount of accumulated evidence before making a choice).

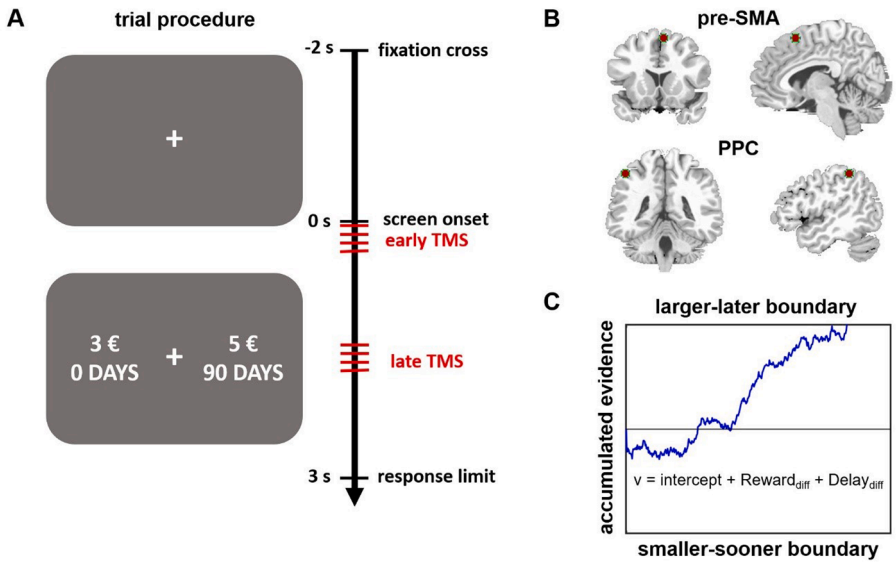

Fig. 1. (A) In an intertemporal decision task, participants made choices between smaller-sooner (e.g., 3 euro today) and larger-later (e.g., 5 euro in 90 days) rewards. Participants performed equal numbers of no TMS, early TMS, and late TMS trials. On early TMS trials, participants received a 10 Hz train of 4 pulses starting 100 ms after decision screen onset. On late TMS, the onset of the pulses was adjusted to the individual median decision time, with the first pulse being administered 300 ms before the individual median. (B) In separate blocks, TMS was administered either to the pre-SMA or to the right PPC. (C) To examine the effects of early versus late TMS on different components of the decision process, we fitted hierarchical Bayesian drift diffusion models to the empirical data. These models assume that, after a non-decision time τ related to perceptual processing, participants accumulate evidence for the two reward options from a starting point ζ (bias parameter) with the velocity ν (drift rate) until the accumulated evidence reaches the decision boundary α.

2.5. Experimental procedure

Upon arrival at the lab, participants were first introduced to the experimental procedures and tasks. After the determination of the indivudal motor threshold (see above), participants performed a practice block with 10 trials of the intertemporal decision task. Participants were seated in a dimly lit room, positioned approximately 60 cm away from the screen, with their chin on a chin rest to maintain a constant viewing distance.

The main experiment comprised a total of 12 blocks, with 6 blocks for the pre-SMA condition and 6 blocks for the PPC condition. Pre-SMA and PPC TMS blocks were presented in randomized order. Each block contained 30 trials, with equal numbers of trials per TMS timing (10 trials no TMS, 10 trials early TMS, 10 trials late TMS). Each experimental block lasted 2.5 minutes and participants were allowed to take breaks between blocks. After the intertemporal decision task, participants were asked to complete a brief questionnaire gathering demographic information.

2.6. Statistical analysis

We analyzed choice data in the intertemporal decision task with model-free and model-based analyses. In all analyses, we considered late TMS trials where no pulse was delivered at least 100 milliseconds before the recorded motor response as no TMS trials to account for the delay in cortico-muscle transmission (Nikolova et al., 2006; Van Acker III et al., 2016).

For the model-free analysis, we computed generalized linear mixed models (GLMMs) with the lme4 package (Bates et al., 2014) in R (version 4.0.0). GLMM-1 regressed binary choices (1 = LL option, 0 = SS option) on fixed-effect predictors for TMS site (pre-SMA versus no TMS and PPC versus no TMS), TMS timing (early versus late), the z-transformed differences in reward magnitudes ($\text{Reward}_{\text{diff}}$) and delays ($\text{Delay}_{\text{diff}}$) between the LL and SS options, and all interaction effects. The fixed effects structure was thus given by the following Eq.:

$$\begin{aligned}(\text{P}(\text{ choice of LL option }) = \beta_0 + \beta_1(\text{ pre}-\text{SMA }) + \beta_2(\text{PPC}) + \beta_3(\text{ pre}-\text{SMA } \times \text{ Timing }) + \\ \beta_4(\textit{PPC} \times \text{ Timing }) + \text{ Reward }_{\text{diff}} \times (\beta_5 + \beta_6(\text{ pre}-\text{SMA }) + \beta_7(\text{PPC}) + \beta_8(\text{ pre}-\text{SMA } \times \text{ Timing }) + \\ \beta_9(\text{PPC} \times \text{ Timing })) + \text{ Delay }_{\text{diff}} \times (\beta_{10} + \beta_{11}(\text{ pre}-\text{SMA }) + \beta_{12}(\text{PPC}) + \beta_{13}(\text{ pre}-\text{SMA } \times \text{ Timing }) + \\ \beta_{14}(\text{PPC} \times \text{ Timing })) + \text{ Reward }_{\text{diff}} \times \text{ Delay }_{\text{diff}} \times (\beta_{15} + \beta_{16}(\text{ pre}-\text{SMA }) + \beta_{17}(\text{PPC}) + \beta_{18}(\text{ pre}- \\ \text{SMA} \times \text{ Timing }) + \beta_{19}(\text{PPC} \times \text{ Timing }))\end{aligned} \quad \text{(Eq. 1)}$$

All fixed-effect predictors were also modelled as random slopes in addition to participant-specific random intercepts. To assess differences between pre-SMA and PPC TMS, we computed GLMM-2 with the same predictors as GLMM-1 but omitting the no TMS trials from the TMS site predictor (pre-SMA versus PPC TMS).

In addition, we analyzed TMS effects on intertemporal choices with Bayesian drift diffusion models (DDM) implemented via the JAGS software package (Plummer, 2003). JAGS uses Markov Chain Monte Carlo sampling to estimate drift diffusion model parameters (drift rate v, boundary α, bias ζ, and non-decision time τ) via the Wiener module (Wabersich and Vandekerckhove, 2014). Choices of SS and LL rewards were associated with lower (negative decision times) and upper (positive decision times) boundaries, respectively. Following previous procedures (Amasino et al., 2019; Soutschek and Tobler, 2023), we assumed that the drift rate v depends on the comparisons of reward magnitudes and delays between the LL and SS options, modulated by factors for TMS site (pre-SMA versus no TMS, PPC versus no TMS) and Timing (early versus late):

$$v = \beta_0 + \beta_1(\text{ pre} - \text{SMA }) + \beta_2(PPC) + \beta_3(\text{ pre} - \text{SMA } \times \text{ Timing }) + \beta_4(PPC \times \text{ Timing }) + \text{Reeward}_{\text{diff}} \times (\beta_5 + \beta_6(\text{ pre} - \text{SMA }) + \beta_7(\text{PPC}) + \beta_8(\text{ pre} - \text{SMA } \times \text{ Timing }) + \beta_9(\text{PPC} \times \text{ Timing })) + \text{Delay}_{\text{diff}} \times (\beta_{10} + \beta_{11}(\text{ pre} - \text{SMA }) + \beta_{12}(\text{PPC}) + \beta_{13}(\text{ pre} - \text{SMA } \times \text{ Timing }) + \beta_{14}(\text{PPC} \times \text{ Timing }))$$ (Eq. 2)

$\text{Reward}_{\text{diff}}$ and $\text{Delay}_{\text{diff}}$ indicate the difference between the reward magnitudes and waiting costs of the LL and SS options, respectively. Pre-SMA and PPC were dummy-coded variables that were set to 1 for pre-SMA and PPC TMS trials, respectively, and to 0 for all other conditions. Timing was coded as -1 for early TMS and +1 for late TMS trials. We note that we modelled no main effect of Timing because in no TMS trials (reference category for which a main effect of Timing would be estimated) there were no early or late TMS pulses as no pulses were delivered at all. In analogy, stimulation effects on the starting bias, decision boundary, and non-decision time were modelled with the following Eq.s:

$$\zeta = \beta_{15} + \beta_{16}(\text{ pre} - \text{SMA }) + \beta_{17}(\text{PPC}) + \beta_{18}(\text{ pre} - \text{SMA } \times \text{ Timing }) + \beta_{19}(\text{PPC} \times \text{ Timing })$$ (Eq. 3)

$$\alpha = \beta_{20} + \beta_{21}(\text{ pre} - \text{SMA }) + \beta_{22}(\text{PPC}) + \beta_{23}(\text{ pre} - \text{SMA } \times \text{ Timing }) + \beta_{24}(\text{PPC} \times \text{ Timing })$$ (Eq. 4)

$$\tau = \beta_{25} + \beta_{26}(\text{ pre} - \text{SMA }) + \beta_{27}(\text{PPC}) + \beta_{28}(\text{ pre} - \text{SMA } \times \text{ Timing }) + \beta_{29}(\text{PPC} \times \text{ Timing })$$ (Eq. 5)

In addition to this first DDM, we also considered a further DDM where the starting bias parameter depended on whether the choice set in a given trial included an immediate reward option:

$$\zeta = \beta_{15} + \beta_{16}(\text{ pre} - \text{SMA }) + \beta_{17}(PPC) + \beta_{18}(\text{ pre} - \text{SMA } \times \text{ Timing }) + \beta_{19}(PPC \times \text{ Timing }) + \text{ Proximity } \times (\beta_{30} + \beta_{31}(\text{ pre} - \text{SMA }) + \beta_{32}(\text{PPC}) + \beta_{33}(\text{ pre} - \text{SMA } \times \text{ Timing }) + \beta_{34}(\text{PPC} \times \text{ Timing }))$$ (Eq. 6)

The variable Proximity represented a dummy-coded factor (0 = no immediate option available, 1 = immediate option available) that allowed us to test the hypothesis that immediate rewards have a proximity advantage over delayed rewards, as reflected by a shift in the starting bias towards the SS decision boundary (Soutschek et al., 2023; Westbrook and Frank, 2018).

In both DDMs, we estimated individual and group-level effects with a hierarchical Bayesian approach, assuming that individual parameter estimates are normally distributed around the group mean. We excluded trials with unreasonable fast decision times below 200 ms to reduce the impact of such trials on parameter estimation. We used normally distributed priors and estimated parameters by computing two chains with 30,000 samples (burning = 25,000). $\widehat{R}$ was $\leq$1.03 for all parameters and even below 1.01 for all group-level parameters, indicating model convergence. We computed Bayes factors (BF_{01}) indicating the evidence for the null hypothesis (effects are zero) relative to the alternative hypothesis (effects differ from zero) using the Savage-Dickey ratio (Wagenmakers et al., 2010). We estimated the density of prior and posterior distributions with the dlogspline function in R.

Lastly, we performed posterior predictive checks both on the group and the individual level by predicting decision times for each participant and trial based on the estimated DDM parameters using the rwiener function in R. We then visually inspected whether the estimated parameters provide a reasonable account of participants' behavior by plotting the estimated against the empirically observed data.

3. Results

First, we assessed the impact of pre-SMA and PPC TMS on intertemporal choices with model-free analyses that did not distinguish between different (temporally separate) subcomponents of the decision process. We regressed binary choices between LL and SS rewards on predictors for TMS site (pre-SMA vs. no TMS and PPC TMS vs. no TMS), Timing (early vs. late TMS), $\text{Reward}_{\text{diff}}$, $\text{Delay}_{\text{diff}}$, and all interaction effects (GLMM-1). On no-TMS trials, participants increasingly preferred the LL over the SS option the larger the magnitude of the LL relative to the SS reward, $\text{Reward}_{\text{diff}}$: Odds Ratio (OR) = 35.53, beta = 3.60, z = 7.71, $p < 0.001$, and the smaller the difference between the delays of the LL and SS option, $\text{Delay}_{\text{diff}}$: OR = 0.50, beta = -0.61, $z = 3.72$, $p < 0.001$, suggesting that our task worked as expected. Next, we analyzed TMS effects on intertemporal choices: Relative to no TMS trials, pre-SMA TMS reduced preferences for LL over SS reward, main effect of pre-SMA TMS: OR = 0.60, beta = -0.56, z = 2.63, p = 0.009, and decreased the sensitivity to reward magnitudes, OR = 0.47, beta = -0.85, $z = 5.19$, $p <$ 0.001 (Fig. 2). A separate GLMM assessing the impact of pre-SMA relative to PPC TMS (GLMM-2) suggests that pre-SMA TMS reduced the sensitivity to rewards also relative to PPC TMS, OR = 1.90, beta = -0.77, z = 3.15, p = 0.002. The interaction between $\text{Reward}_{\text{diff}}$ and $\text{Delay}_{\text{diff}}$ was differently affected by early versus late PPC TMS relative to no TMS (GLMM-1), OR = 0.75, beta = -0.34, $z = 3.52$, $p < 0.001$, and at trend-level relative to pre-SMA TMS (GLMM-2), OR = 0.75, beta = -0.32, z = 1.90, p = 0.06. Separate GLMMs (GLMM-3) for early versus late PPC TMS pulses, however, revealed no evidence for significant effects of early or late PPC TMS on the $\text{Reward}_{\text{diff}} \times \text{Delay}_{\text{diff}}$ interaction, both $p > 0.12$. Taken together, these GLMMs suggest that pre-SMA TMS impairs the sensitivity to differences in reward magnitude independently of the timing of TMS pulses, whereas the PPC might affect intertemporal decisions differently at later compared with earlier periods of the decision process. However, these model-free analyses are agnostic to which subcomponents of the decision process are influenced by the pre-SMA and the PPC.

To obtain a deeper understanding of the computational mechanisms underlying the pre-SMA's contribution to intertemporal choice, we computed hierarchical Bayesian DDMs where the drift rate v was given by the weighted influences of differences in reward magnitudes and delays in addition to participant-specific intercepts. Consistent with previous research (Soutschek and Tobler, 2023), a DDM where the starting bias parameter was additionally modulated by a proximity bias (different starting biases for immediate versus delayed SS rewards) explained the data better (DIC = 8708) than a model without proximity bias (DIC = 8846). Posterior predictive checks comparing simulated with observed data suggest that the DDM with proximity bias provided a reasonable account of the data (Fig. 3 and Fig. S1). In this model, larger LL than SS rewards were associated with evidence accumulation towards the boundary for the LL option, β_5: HDI_{mean} = 0.84, $\text{HDI}_{95\%}$ = [0.66, 1.02], $BF_{01} = 2.3 \times 10^{-8}$, whereas larger differences in delay resulted in faster accumulation towards the SS boundary, β_{10}: HDI_{mean} = -0.22, $\text{HDI}_{95\%}$ = [-0.32, -0.12], BF_{01} = 0.005. Pre-SMA TMS lowered the sensitivity to rewards compared to both no TMS, β_6: HDI_{mean} = -0.08, $\text{HDI}_{95\%}$ = [-0.15, -0.01], BF_{01} = 2.3, and PPC TMS (direct comparison of posterior samples between pre-SMA and PPC TMS), HDI_{mean} = -0.11, $\text{HDI}_{95\%}$ = [-0.20, -0.02], BF_{01} = 0.98 (Fig. 4 and Fig. S2). In addition, pre-SMA perturbation reduced the drift rate intercept parameter (biasing evidence accumulation towards the SS boundary), again

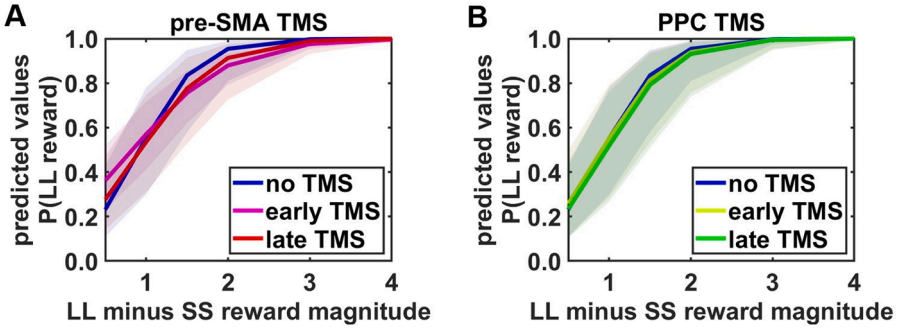

Fig. 2. Model-free results. (A) Inhibitory pre-SMA TMS (independently of pulse timing) reduced the sensitivity to differences in reward magnitudes compared to no TMS and PPC TMS trials. (B) PPC TMS, in contrast, did not alter reward sensitivity relative to pre-SMA TMS. Shaded areas show 95% confidence interval for the predicted probabilities of choosing the larger-later (LL) over smaller-sooner (SS) reward.

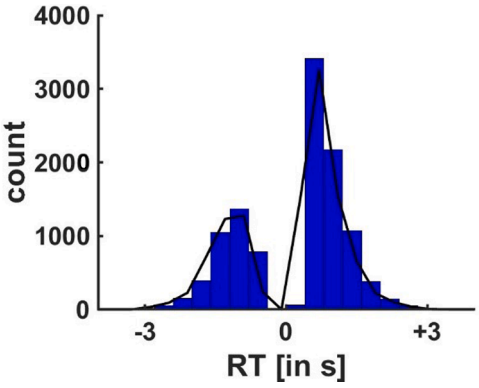

Fig. 3. Posterior predictive checks revealed strong overlap between empirical data (blue histogram) and data simulated based on the best-fitting drift diffusion model (black line).

relative to both no TMS, β_1: HDI_{mean} = -0.16, $HDI_{95\%}$ = [-0.29, -0.04], BF_{01} = 0.6, and (comparison of posterior samples between pre-SMA and PPC TMS) PPC TMS trials, HDI_{mean} = -0.15, $HDI_{95\%}$ = [-0.30, -0.02], BF_{01} =1.3. Note that these effects should be interpreted with caution given that (although the $HDIs_{95\%}$ do not include zero) the Bayes factors provide no clear evidence in favor of the alternative hypothesis. We observed no evidence for an influence of PPC TMS on drift rate parameters, and there were also no significant interactions of pre-SMA or PPC TMS with the timing of TMS pulses (Table 2). PPC TMS lowered decision boundaries relative to no TMS, β_{22}: HDI_{mean} = -0.10, $HDI_{95\%}$ = [-0.19, -0.01], BF_{01} = 1.8, but not relative to pre-SMA TMS (comparison of posterior samples between pre-SMA and PPC TMS), HDI_{mean} = -0.06, $HDI_{95\%}$ = [-0.17, 0.05], BF_{01} = 11.0. Moreover, compared with no TMS trials both pre-SMA and PPC TMS prolonged decision times, particularly for late versus early pulses, pre-SMA × Timing (β_{28}:): HDI_{mean} = 0.04, $HDI_{95\%}$ = [0.02, 0.07], BF_{01} = 0.2, PPC × Timing (β_{29}:): HDI_{mean} = 0.06, $HDI_{95\%}$ = [0.04, 0.09], BF_{01} = 0.005. However, as these effects did not differ between pre-SMA and PPC TMS (comparison of posterior samples between pre-SMA and PPC TMS), HDI_{mean} = -0.02, $HDI_{95\%}$ = [-0.05, 0.01], BF_{01} = 31.3, they may represent site-unspecific effect of late TMS pulses due to interference with motor execution processes.

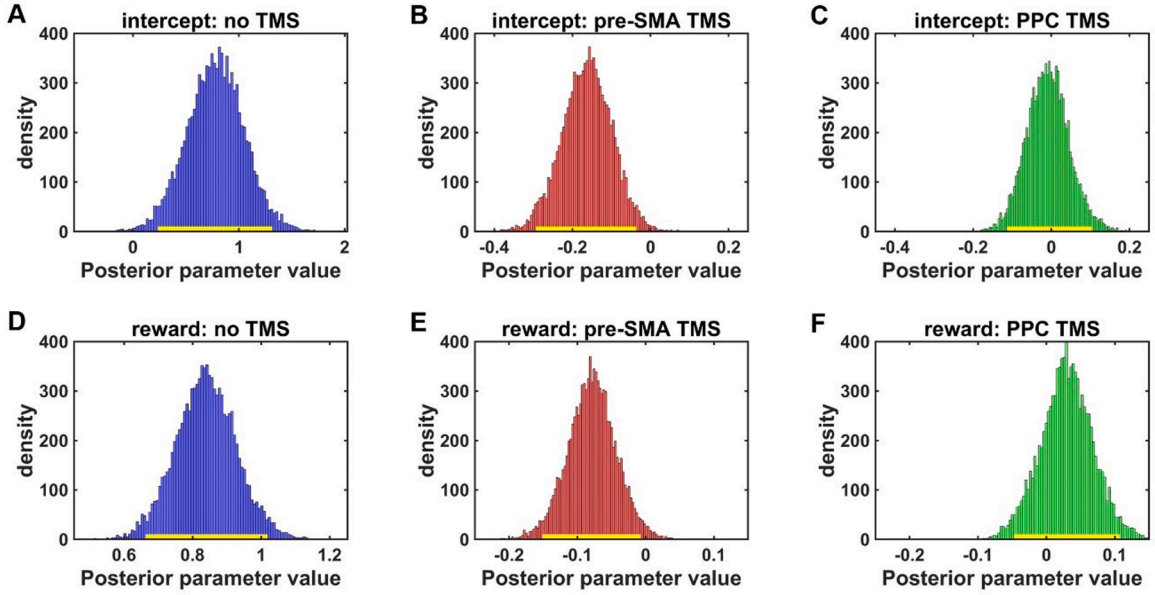

Fig. 4. Results of Bayesian drift diffusion model. (A) Participants generally tended to accumulate evidence faster towards the boundary for LL than for SS choices, indicated by a positive intercept of the drift rate on no TMS trials (parameter β_0 in proximity DDM). (B) Pre-SMA TMS, relative to no TMS, reduced the intercept parameter of the drift rate (parameter β_1), whereas (C) PPC TMS showed no significant effects relative to no TMS (parameter β_2). (D) Larger differences in reward magnitude were associated with stronger evidence accumulation towards the LL boundary in no TMS trials (parameter β_5). (E) Compared to no TMS trials, pre-SMA TMS lowered the sensitivity to differences in reward magnitude (parameter β_6), whereas (F) PPC TMS showed no significant effect (parameter β_7).

Table 1
Results of model-free generalized linear mixed model (GLMM-1) on binary decisions (1 = larger-later reward, 0 = smaller-sooner reward) in the intertemporal choice task. Standard errors of the mean are in brackets.

Effect	Beta	z	p
Intercept	3.14 (0.84)	3.74	<0.001
pre-SMA TMS	-0.56 (0.22)	2.63	0.009
PPC TMS	-0.16 (0.12)	1.36	0.17
pre-SMA TMS × Timing	0.02 (0.08)	0.22	0.83
PPC TMS × Timing	-0.07 (0.09)	0.83	0.41
$Reward_{diff}$	3.60 (0.47)	7.71	<0.001
$Delay_{diff}$	-0.61 (0.16)	3.72	<0.001
pre-SMA TMS × $Reward_{diff}$	-0.85 (0.16)	5.19	<0.001
PPC TMS × $Reward_{diff}$	-0.09 (0.16)	0.60	0.55
pre-SMA TMS × $Delay_{diff}$	-0.14 (0.14)	0.97	0.33
PPC TMS × $Delay_{diff}$	-0.05 (0.10)	0.44	0.66
pre-SMA TMS × Timing × $Reward_{diff}$	0.07 (0.10)	0.80	0.42
PPC TMS × Timing × $Reward_{diff}$	-0.08 (0.09)	0.87	0.39
pre-SMA TMS × Timing × $Delay_{diff}$	0.08 (0.08)	0.98	0.33
PPC TMS × Timing × $Delay_{diff}$	-0.26 (0.11)	2.31	0.02
$Reward_{diff}$ × $Delay_{diff}$	-0.00 (0.12)	0.00	1.00
pre-SMA TMS × $Reward_{diff}$ × $Delay_{diff}$	-0.23 (0.13)	1.77	0.08
PPC TMS × $Reward_{diff}$ × $Delay_{diff}$	0.10 (0.14)	0.72	0.47
pre-SMA TMS × Timing × $Reward_{diff}$ × $Delay_{diff}$	0.07 (0.09)	0.77	0.44
PPC TMS × Timing × $Reward_{diff}$ × $Delay_{diff}$	-0.34 (0.10)	3.52	<0.001

Table 2
Results of hierarchical Bayesian drift diffusion model. We report the mean highest density interval (HDI) as well as the upper and lower limits of the 95% HDI.

Parameter	Effect	HDI_{mean}	$HDI_{2.5\%}$	$HDI_{97.5\%}$
Drift: intercept	no TMS	0.78	0.24	1.31
	pre-SMA TMS	-0.16	-0.29	-0.04
	PPC TMS	-0.01	-0.11	0.10
	pre-SMA TMS × Timing	-0.00	-0.07	0.07
	PPC TMS × Timing	-0.04	-0.12	0.03
Drift: $Reward_{diff}$	no TMS	0.84	0.66	1.02
	pre-SMA TMS	-0.08	-0.15	-0.01
	PPC TMS	0.03	-0.05	0.11
	pre-SMA TMS × Timing	0.04	-0.04	0.12
	PPC TMS × Timing	-0.01	-0.07	0.05
Drift: $Delay_{diff}$	no TMS	-0.22	-0.32	-0.12
	pre-SMA TMS	-0.04	-0.10	0.03
	PPC TMS	-0.03	-0.10	0.04
	pre-SMA TMS × Timing	-0.02	-0.07	0.03
	PPC TMS × Timing	0.00	-0.05	0.06
Bias: intercept	no TMS	0.52	0.50	0.55
	pre-SMA TMS	0.01	-0.01	0.02
	PPC TMS	-0.01	-0.04	0.01
	pre-SMA TMS × Timing	-0.00	-0.02	0.02
	PPC TMS × Timing	-0.00	-0.03	0.01
Bias: proximity	no TMS	-0.02	-0.04	0.01
	pre-SMA TMS	0.01	-0.01	0.04
	PPC TMS	0.01	-0.02	0.03
	pre-SMA TMS × Timing	0.01	-0.01	0.03
	PPC TMS × Timing	0.01	-0.01	0.03
Decision boundary	no TMS	2.00	1.87	1.12
	pre-SMA TMS	-0.05	-0.12	0.03
	PPC TMS	-0.10	-0.19	-0.01
	pre-SMA TMS × Timing	-0.01	-0.05	0.04
	PPC TMS × Timing	-0.02	-0.07	0.04
Non-decision time	no TMS	0.44	0.39	0.49
	pre-SMA TMS	0.06	0.03	0.09
	PPC TMS	0.09	0.05	0.13
	pre-SMA TMS × Timing	0.04	0.02	0.07
	PPC TMS × Timing	0.06	0.04	0.09

As robustness check, we controlled whether this result pattern holds for the (worse fitting) DDM without proximity parameter. This analysis replicated the effects of pre-SMA TMS on the drift rate intercept, HDI_{mean} = -0.80, $HDI_{95\%}$ = [-0.16, -0.01], BF_{01} = 0.5, and on the sensitivity to rewards, HDI_{mean} = -0.16, $HDI_{95\%}$ = [-0.29, -0.04], BF_{01} = 3.0. Taken together, the DDM results inform the model-free findings by showing that the pre-SMA influences the sensitivity to reward magnitude in intertemporal decision making.

4. Discussion

While neural accounts of cost-benefit decision-making predominantly focus on the DLPFC as neural substrate of cognitive control, the contributions of other parts of the frontoparietal control network have been neglected so far. Here, we provide evidence for a causal role of the pre-SMA for evidence accumulation in intertemporal decisions: according to our model-free analyses, pre-SMA perturbation during decision making reduced the sensitivity to larger compared with smaller rewards, suggesting a role of the pre-SMA for promoting patient decisions, in analogy to the DLPFC's role in intertemporal choice (Smith et al., 2018; Wesley and Bickel, 2014; Yang et al., 2018). However, from these model-free analyses alone it remains unclear which component of the decision process was affected by pre-SMA TMS. From a process perspective, TMS-induced changes in patience could be explained either by a shift in the starting bias towards the SS reward boundary, by changes in the amount of evidence required to make a choice (decision boundary), or by slower evidence accumulation towards LL rewards. Our hierarchical Bayesian DDMs support the third hypothesis: Disrupting pre-SMA activation lowered the general speed of the evidence accumulation process towards the decision boundary for LL rewards (intercept of drift rate) and reduced the sensitivity to rewards, while leaving the starting point of the accumulation process or the height of the decision boundary unchanged. Thus, the pre-SMA influences intertemporal decision making by strengthening the preference for costly larger rewards. This reveals the computational role of the pre-SMA for cost-benefit weighing in intertemporal choice, a brain region that so far has been neglected in neural accounts of intertemporal choice. The pre-SMA appears to promote patience in a similar way as the DLPFC whose causal contribution to intertemporal choice is evidenced by a large body of evidence (Yang et al., 2018). However, while the DLPFC is thought to promote patience by representing abstract information in working memory like the value of long-term rewards or goals (Jimura et al., 2018), pre-SMA was linked to control over response selection processes and may itself receive input from DLPFC (Badre and Nee, 2018). We therefore speculate that DLPFC and pre-SMA may play dissociable functional roles in intertemporal choice.

Past DDMs of pre-SMA's function in value-based decisions assigned it a role for tracking the evidence accumulated for reward options (Pisauro et al., 2017; Rodriguez et al., 2014). However, due to the correlative nature of neuroimaging findings, these results left open whether pre-SMA passively reflects the evidence accumulated so far, or whether pre-SMA influences the evidence accumulation process itself. Moreover, other studies related the pre-SMA to the height of the decision boundaries (Berkay et al., 2018) or to the starting bias parameter (McIntosh and Sajda, 2020). By combining brain stimulation with computational modelling, we clarify the pre-SMA's computational role for value-based choice and provide evidence that the pre-SMA does not only track the evidence for the choice options but enhances the velocity of the accumulation process for larger relative to smaller rewards. We note that in a previous study on effort-based decision making we found that excitatory transcranial electrical stimulation over pre-SMA shifted the starting bias towards large effortful rewards (Soutschek et al., 2022), but the stimulation setup in this study was less spatially precise and affected also deeper regions like anterior cingulate cortex (via placing a reference electrode under the chin that induced a current flow through the brain). Given the higher spatial resolution of TMS, the current findings suggest that pre-SMA strengthens the preference for larger rewards in the domain of intertemporal choices.

Note that the pre-SMA is likely to promote patient decisions not in isolation but as part of a network comprising several regions involved in decision making. As pre-SMA shows fiber connections with the striatum (Bozkurt et al., 2016), pre-SMA activation might moderate the

sensitivity to rewards via influencing striatal reward representations, in analogy to the hypothesized role of DLPFC for intertemporal choice (van den Bos et al., 2014). It is therefore important to keep in mind that neural manipulations affect not only local processing in the targeted area but also influence activation in functionally interconnected regions (Bergmann et al., 2021; Riddle et al., 2022).

Contrary to our hypotheses, we found no significant effects of PPC perturbation on evidence accumulation. If anything, late PPC TMS may have lowered the height of the decision boundary (in addition to site-unspecific effects on the non-decision time, presumably due to effects on TMS-induced arousal on motor execution). The lack of significant effects of PPC stimulation on decision making may appear surprising given that previous imaging studies reported PPC activation during intertemporal decisions (Rodriguez et al., 2014; van den Bos et al., 2014; Wesley and Bickel, 2014). We emphasize that our null finding does not necessarily imply that PPC does not causally contribute to intertemporal decisions, and it remains possible that other subregions of parietal cortex influence decision making. In fact, more ventral regions, in particular the temporo-parietal junction, were related to patient intertemporal decision making (Lempert et al., 2017; Soutschek et al., 2020; Soutschek et al., 2016). In any case, while the PPC was shown to be causally involved in other domains of decision making like decisions under ambiguity (Studer et al., 2014; Valdebenito-Oyarzo et al., 2024), the current data provide no evidence for a causal contribution of PPC to intertemporal choice.

While the current investigation has several strengths like the combination of time-locked neuronavigated TMS with Bayesian computational modelling, a potential limitation is that online TMS can be perceived as aversive by participants, which can lead to site-unspecific influences on behavior. It is important to note that the pre-SMA and the PPC are thought to show similar TMS-induced discomfort (Meteyard and Holmes, 2018) and that we interpret only pre-SMA TMS effects that were significant compared to both no TMS and PPC TMS as active control condition. It is thus unlikely that TMS-induced discomfort can explain the impact of pre-SMA stimulation on evidence accumulation.

Taken together, the current results provide insights into the computational role of the pre-SMA for intertemporal decision making, a region that has received little attention in previous research on cost-benefit decision making. This finding may also improve our understanding of the neural origins of increased impulsiveness in clinical disorders: While neural interventions for the treatment of impulsiveness deficits in clinical disorders like addiction mainly targeted the DLPFC (Azevedo and Mammis, 2018; Dunlop et al., 2017), impulsiveness in substance addiction was also related to pre-SMA dysfunctioning (Quoilin et al., 2021). The current findings suggest that the pre-SMA might represent an alternative promising target for neural interventions against the impulsiveness deficits in disorders like substance dependence.

Data and code availability statement

The raw data and the analysis code are publically available on the Open Science Framework (OSF; https://osf.io/jn62v/?view_only=793c74e55fc04681aaa2a506bf322e60).

CRediT authorship contribution statement

Gizem Vural: Conceptualization, Formal analysis, Investigation, Validation, Writing – original draft. **Natasha Katruss:** Conceptualization, Formal analysis, Investigation, Writing – review & editing. **Alexander Soutschek:** Conceptualization, Formal analysis, Funding acquisition, Supervision, Visualization, Writing – original draft.

Declaration of competing interest

The authors declare to have no conflicts of interest.

Acknowledgements

AS received support from an Emmy Noether fellowship of the German Research Foundation (SO 1636/2-1) and an Exploration grant from the Boehringer Ingelheim Foundation.

Supplementary materials

Supplementary material associated with this article can be found, in the online version, at doi:10.1016/j.neuroimage.2024.120838.

Literature

Amasino, D.R., Sullivan, N.J., Kranton, R.E., Huettel, S.A., 2019. Amount and time exert independent influences on intertemporal choice. Nat. Hum. Behav. 3, 383–392.
Arabadzhiyska, D.H., Garrod, O.G.B., Fouragnan, E., De Luca, E., Schyns, P.G., Philiastides, M.G., 2022. A Common Neural Account for Social and Nonsocial Decisions. J. Neurosci. 42, 9030–9044.
Azevedo, C.A., Mammis, A., 2018. Neuromodulation therapies for alcohol addiction: a literature review. Neuromodulation: Technology at the Neural Interface 21, 144–148.
Badre, D., Nee, D.E., 2018. Frontal Cortex and the Hierarchical Control of Behavior. Trends. Cogn. Sci. 22, 170–188.
Bates, D., Mächler, M., Bolker, B., Walker, S., 2014. Fitting linear mixed-effects models using lme4. arXiv preprint arXiv:1406.5823.
Bergmann, T.O., Varatheeswaran, R., Hanlon, C.A., Madsen, K.H., Thielscher, A., Siebner, H.R., 2021. Concurrent TMS-fMRI for causal network perturbation and proof of target engagement. Neuroimage 237, 118093.
Berkay, D., Eser, H.Y., Sack, A.T., Cakmak, Y.O., Balci, F., 2018. The modulatory role of pre-SMA in speed-accuracy tradeoff: A bi-directional TMS study. Neuropsychologia 109, 255–261.
Bozkurt, B., Yagmurlu, K., Middlebrooks, E.H., Karadag, A., Ovalioglu, T.C., Jagadeesan, B., Sandhu, G., Tanriover, N., Grande, A.W., 2016. Microsurgical and Tractographic Anatomy of the Supplementary Motor Area Complex in Humans. World Neurosurg. 95, 99–107.
Dunlop, K., Hanlon, C.A., Downar, J., 2017. Noninvasive brain stimulation treatments for addiction and major depression. Ann. N. Y. Acad. Sci. 1394, 31–54.
Erlich, J.C., Brunton, B.W., Duan, C.A., Hanks, T.D., Brody, C.D., 2015. Distinct effects of prefrontal and parietal cortex inactivations on an accumulation of evidence task in the rat. Elife 4, e05457.
Frost, R., McNaughton, N., 2017. The neural basis of delay discounting: A review and preliminary model. Neurosci. Biobehav. Rev. 79, 48–65.
Jimura, K., Chushak, M.S., Westbrook, A., Braver, T.S., 2018. Intertemporal Decision-Making Involves Prefrontal Control Mechanisms Associated with Working Memory. Cereb. Cortex. 28, 1105–1116.
Kapetaniou, G.E., Reinhard, M.A., Christian, P., Jobst, A., Tobler, P.N., Padberg, F., Soutschek, A., 2021. The role of oxytocin in delay of gratification and flexibility in non-social decision making. Elife 10.
Krueger, P.M., van Vugt, M.K., Simen, P., Nystrom, L., Holmes, P., Cohen, J.D., 2017. Evidence accumulation detected in BOLD signal using slow perceptual decision making. J. Neurosci. Methods 281, 21–32.
Lempert, K.M., Speer, M.E., Delgado, M.R., Phelps, E.A., 2017. Positive autobiographical memory retrieval reduces temporal discounting. Soc. Cogn. Affect. Neurosci. 12, 1584–1593.
McClure, S.M., Laibson, D.I., Loewenstein, G., Cohen, J.D., 2004. Separate neural systems value immediate and delayed monetary rewards. Science (1979) 306, 503–507.
McIntosh, J.R., Sajda, P., 2020. Decomposing Simon task BOLD activation using a drift-diffusion model framework. Sci. Rep. 10, 3938.
Meteyard, L., Holmes, N.P., 2018. TMS SMART–scalp mapping of annoyance ratings and twitches caused by transcranial magnetic stimulation. J. Neurosci. Methods 299, 34–44.
Nikolova, M., Pondev, N., Christova, L., Wolf, W., Kossev, A.R., 2006. Motor cortex excitability changes preceding voluntary muscle activity in simple reaction time task. Eur. J. Appl. Physiol. 98, 212–219.
Pisauro, M.A., Fouragnan, E., Retzler, C., Philiastides, M.G., 2017. Neural correlates of evidence accumulation during value-based decisions revealed via simultaneous EEG-fMRI. Nat. Commun. 8, 15808.
Plummer, M., 2003. JAGS: A program for analysis of Bayesian graphical models using Gibbs sampling. In: Proceedings of the 3rd international workshop on distributed statistical computing. Vienna, Austria, pp. 1–10.
Quoilin, C., Dricot, L., Genon, S., de Timary, P., Duque, J., 2021. Neural bases of inhibitory control: Combining transcranial magnetic stimulation and magnetic resonance imaging in alcohol-use disorder patients. Neuroimage 224, 117435.
Ratcliff, R., Smith, P.L., Brown, S.D., McKoon, G., 2016. Diffusion Decision Model: Current Issues and History. Trends. Cogn. Sci. 20, 260–281.
Riddle, J., Scimeca, J.M., Pagnotta, M.F., Inglis, B., Sheltraw, D., Muse-Fisher, C., D'Esposito, M., 2022. A guide for concurrent TMS-fMRI to investigate functional brain networks. Front. Hum. Neurosci. 16, 1050605.
Rochas, V., Gelmini, L., Krolak-Salmon, P., Poulet, E., Saoud, M., Brunelin, J., Bediou, B., 2013. Disrupting pre-SMA activity impairs facial happiness recognition: an event-related TMS study. Cereb. Cortex. 23, 1517–1525.

Rodriguez, C.A., Turner, B.M., McClure, S.M., 2014. Intertemporal choice as discounted value accumulation. PLoS. One 9, e90138.
Smith, B.J., Monterosso, J.R., Wakslak, C.J., Bechara, A., Read, S.J., 2018. A meta-analytical review of brain activity associated with intertemporal decisions: Evidence for an anterior-posterior tangibility axis. Neurosci. Biobehav. Rev. 86, 85–98.
Soutschek, A., Jetter, A., Tobler, P.N., 2023. Toward a Unifying Account of Dopamine's Role in Cost-Benefit Decision Making. Biol. Psychiatry Glob. Open. Sci. 3, 179–186.
Soutschek, A., Moisa, M., Ruff, C.C., Tobler, P.N., 2020. The right temporoparietal junction enables delay of gratification by allowing decision makers to focus on future events. PLoS. Biol. 18, e3000800.
Soutschek, A., Nadporozhskaia, L., Christian, P., 2022. Brain stimulation over dorsomedial prefrontal cortex modulates effort-based decision making. Cogn. Affect. Behav. Neurosci. 22, 1264–1274.
Soutschek, A., Ruff, C.C., Strombach, T., Kalenscher, T., Tobler, P.N., 2016. Brain stimulation reveals crucial role of overcoming self-centeredness in self-control. Sci. Adv. 2, e1600992.
Soutschek, A., Tobler, P.N., 2023. A process model account of the role of dopamine in intertemporal choice. Elife 12, e83734.
Studer, B., Cen, D., Walsh, V., 2014. The angular gyrus and visuospatial attention in decision-making under risk. Neuroimage 103, 75–80.
Taylor, P.C., Muggleton, N.G., Kalla, R., Walsh, V., Eimer, M., 2011. TMS of the right angular gyrus modulates priming of pop-out in visual search: combined TMS-ERP evidence. J. Neurophysiol. 106, 3001–3009.
Taylor, P.C., Nobre, A.C., Rushworth, M.F., 2007. Subsecond changes in top down control exerted by human medial frontal cortex during conflict and action selection: a combined transcranial magnetic stimulation electroencephalography study. J. Neurosci. 27, 11343–11353.
Thut, G., Veniero, D., Romei, V., Miniussi, C., Schyns, P., Gross, J., 2011. Rhythmic TMS causes local entrainment of natural oscillatory signatures. Curr. Biol. 21, 1176–1185.
Valdebenito-Oyarzo, G., Martínez-Molina, M.P., Soto-Icaza, P., Zamorano, F., Figueroa-Vargas, A., Larraín-Valenzuela, J., Stecher, X., Salinas, C., Bastin, J., Valero-Cabré, A., 2024. The parietal cortex has a causal role in ambiguity computations in humans. PLoS. Biol. 22, e3002452.
Van Acker III, G.M., Luchies, C.W., Cheney, P.D., 2016. Timing of cortico-muscle transmission during active movement. Cerebral Cortex 26, 3335–3344.
van den Bos, W., Rodriguez, C.A., Schweitzer, J.B., McClure, S.M., 2014. Connectivity strength of dissociable striatal tracts predict individual differences in temporal discounting. J. Neurosci. 34, 10298–10310.
Wabersich, D., Vandekerckhove, J., 2014. Extending JAGS: A tutorial on adding custom distributions to JAGS (with a diffusion model example). Behav. Res. Methods 46, 15–28.
Wagenmakers, E.J., Lodewyckx, T., Kuriyal, H., Grasman, R., 2010. Bayesian hypothesis testing for psychologists: a tutorial on the Savage-Dickey method. Cogn. Psychol. 60, 158–189.
Wagner, B., Clos, M., Sommer, T., Peters, J., 2020. Dopaminergic Modulation of Human Intertemporal Choice: A Diffusion Model Analysis Using the D2-Receptor Antagonist Haloperidol. Journal of Neuroscience 40, 7936–7948.
Wesley, M.J., Bickel, W.K., 2014. Remember the future II: meta-analyses and functional overlap of working memory and delay discounting. Biol. Psychiatry 75, 435–448.
Westbrook, A., Frank, M., 2018. Dopamine and Proximity in Motivation and Cognitive Control. Curr. Opin. Behav. Sci. 22, 28–34.
Yang, C.C., Vollm, B., Khalifa, N., 2018. The Effects of rTMS on Impulsivity in Normal Adults: a Systematic Review and Meta-Analysis. Neuropsychol. Rev. 28, 377–392.
Yu, Q., Panichello, M.F., Cai, Y., Postle, B.R., Buschman, T.J., 2020. Delay-period activity in frontal, parietal, and occipital cortex tracks noise and biases in visual working memory. PLoS. Biol. 18, e3000854.
Zhang, Z., Yin, C., Yang, T., 2022. Evidence accumulation occurs locally in the parietal cortex. Nat. Commun. 13, 4426.